On the propagation and modulation of electrostatic solitary waves observed near the magnetopause on Cluster

J. S. Pickett[1], I. W. Christopher[1], B. Grison[2], M. J. Engebretson[3], S. Grimald[4], O. Santolík[2,5], P. M. E. Décréau[6], L. Kistler[7], D. Constantinescu[8], B. Lefebvre[7], L.-J. Chen[7], Y. Omura[9], G. S. Lakhina[10], D. A. Gurnett[1], N. Cornilleau-Wehrlin[11], A. N. Fazakerley[12], I. Dandouras[4], and E. Lucek[13]

[1] Department of Physics and Astronomy, The University of Iowa, Iowa City, IA, USA
[2] Institute of Atmospheric Physics, Prague, Czech Republic
[3] Dept. of Physics, Augsburg College, Minneapolis, MN, USA
[4] Université de Toulouse and CESR, Toulouse, France
[5] Charles University, Faculty of Mathematics and Physics, Prague, Czech Republic
[6] LPC2E, CNRS et Université d'Orléans, Orléans, France
[7] Space Science Center, University of New Hampshire, Durham, NH, USA
[8] TU, Braunschweig, Germany
[9] Research Institute for Sustainable Humanosphere, Kyoto University, UJI, Kyoto, Japan
[10] Upper Atmospheric Studies, Indian Institute of Geomagnetism, Navi Mumbai, India
[11] Station de Radioastronomie de Nançay, Observatoire de Paris, CNRS, Nançay, France
[12]Mullard Space Science Laboratory, Holmbury St. Mary, UK
[13] Imperial College, London, UK

Abstract. We present the results of a study of Electrostatic Solitary Waves (ESWs) in which propagation of a series of noncyclical ESWs is observed from one Cluster spacecraft to another over distances as great as tens of km and time lags as great as a few tens of ms. This propagation study was conducted for locations near the magnetopause on the magnetosheath side. Propagation was found primarily toward the earth with speeds on the order of 1500 to 2400 km/s. The sizes of the ESWs obtained from these velocities were on the order of 1 km along the magnetic field direction and several tens of km perpendicular (i.e., pancake shaped). These results are consistent with measurements on single spacecraft in which the ESW propagation is observed with time lags of only ~ 0.1 ms. Our results thus show the stability of ESWs over time periods much greater than their own characteristic pulse durations of a few 100s of microseconds. We present also the results of a study of ESW modulation at the magnetopause on the earthward side. We found that ESWs were modulated at ~ 1.3 Hz, consistent with a Pc1 wave which was observed concurrently. During this time, tens of eV electron beams are present. We propose a Buneman type instability in which the $E_{//}$ component of the Pc1 waves provides a mechanism for accelerating electrons, resulting in the generation of the ESWs modulated at the Pc1 frequency.

1. Introduction

Electrostatic Solitary Waves (ESWs) have been highly studied since their first observations in the data of S3-3 (Temerin et al., 1982) and with the advent in the 1990s of digital high time resolution waveform receivers mounted on spacecraft (c.f., Matsumoto et al., 1994). ESWs are generally observed in these waveform data as isolated pulses and as a series of cyclic or noncyclic pulses or wavepackets, usually with similar amplitudes and pulse time durations. They are usually found in regions of space which are turbulent or in which there are mixing of plasmas, such as in and near boundary layers and along auroral field lines (Pickett et al., 2004a). Much of the past work, both observational and theoretical, on ESWs and their association with electron phase space holes, has been discussed by Franz et al. (2005) in the introduction to their work on the properties of small-amplitude electron phase-space holes observed

on the Polar spacecraft. In additional Ghosh et al. (2008) also reviewed many of the past ESW studies in the introduction to their work on electron acoustic solitary waves in a magnetized plasma with application to boundary layers. ESWs are almost always found in and near the magnetopause and its boundary as first reported by Cattell et al. (2002) through Polar observations at the subsolar, equatorial magnetopause. The ESWs in this region were reported by them to have amplitudes up to ~ 25 mV/m and velocities from ~ 150 km/s to > 2000 km/s with scale sizes on the order of a kilometer (comparable to the Debye length). ESWs and amplitude modulated electrostatic waves (AMEWs) were later found by Matsumoto et al. (2003) to be associated with 3-dimensional reconnection using data from GEOTAIL as the spacecraft skimmed along the dayside magnetopause. They showed that the ESWs and AMEWs were not random noises but rather nonlinear coherent structures, possibly providing dissipation in the electron diffusion region.

In the present study, we use data obtained on the Cluster spacecraft near the magnetopause boundary layer (MPBL) to further our understanding of ESWs in this very dynamic region. We first present data relating to the propagation of ESWs close to the magnetopause on the magnetosheath side. For this study, we use the multi-spacecraft aspect of Cluster to determine ESW propagation speed and size. The results of this study are presented in Section 2. We follow this in Section 3 with a study of ESWs which are observed to occur in bursts modulated at a low frequency of approximately 1.3 Hz. The Cluster observations presented in Sections 2 and 3 were obtained by the Wideband Data (WBD) plasma wave receiver (Gurnett et al., 1997), the Spatio-Temporal Analysis of Field Fluctuations Search Coil (STAFF-SC) and Spectrum Analyzer (STAFF-SA) instruments (Cornilleau-Wehrlin et al., 2003), the Fluxgate Magnetometer (FGM) (Balogh et al., 1997), and the WHISPER resonance sounder and wave analyzer (Décréau et al., 1997). In Section 4 we discuss the significance of the observations contained in Sections 2 and 3 with respect to the physical processes that are likely to be behind the generation of the ESWs and their modulation. In addition for the ESW modulation event we discuss the characteristics of the electrons using the PEACE data (Johnstone et al., 1997) and of the ions using the CIS data (Rème et al. 2001). Finally, we summarize our results and present some basic conclusions in Section 5.

2. Propagation of ESWs

Prior to the launch of Cluster, spacecraft observations of the propagation of ESWs near the magnetopause were constrained to a single spacecraft. The technique of observing and determining propagation involved the use of interferometry. A dipole antenna, which spans the length from one probe to another through the spacecraft body, is divided into two antennas with the spacecraft body acting as the end probe for each of the two. An ESW is first detected by one of these two antennas. The delay between that measurement and the detection of the ESW at the second antenna is then used, together with the known antenna lengths, to get the propagation speed (c.f., Franz et al., 1998). The measurements are usually oriented with respect to the background magnetic field to determine if the propagation was along the field or at some angle off this direction. In most cases, the ESWs are seen propagating along the magnetic field direction, either parallel or anti-parallel. However, the maximum distance traveled by ESWs with these measurements was limited by the length of the antennas, thus being on the order of 50 m. With the advent of Cluster, it was now possible to consider propagation from one spacecraft to another. There have been two documented cases of ESW propagation on Cluster: 1) along auroral field lines at a distance of 4.8 R_E on the nightside (Pickett et al., 2004b), and 2) in the dayside magnetopause boundary layer at a distance of 11.9 R_E on the magnetosheath side (Pickett et al., 2008). The method for determination of cross spacecraft propagation is a complex and time consuming process of defining the shape (time and amplitude) characteristics of the ESWs, using a computer program to search for these signatures in the data from each spacecraft, and then cross-correlating the ESW detections across the various spacecraft using a series of irregularly spaced ESWs (see Pickett et al. (2004b; 2008) for more details on this method). In Figure 1, which we have extracted from Figure 5 of Pickett et al. (2008), we show the 8 ms waveforms from Cluster spacecraft 4 (SC4) as a black line with the waveforms from SC3 overlaid as a

green line and brought forward in time by its lag to SC4 by 22.49 ms. The agreement is quite striking and shows that it is possible for ESWs to be stable over a 22 ms time span, allowing for the calculation of the propagation speed and size of the ESWs similar to the method employed on one spacecraft.

Using this same method, a few other cases of propagation in the MPBL on the magnetosheath side were found in the Cluster data set in the only period of time when the Cluster spacecraft were on the dayside near the MPBL and the spacecraft were close enough to observe the propagation. This was the approximate February through May 2002 period when the inter-spacecraft separations were on the order of 100 km, with a perfect tetrahedron targeted for the northern cusp. Table 1 shows the spacecraft locations and ESW propagation characteristics for the six documented cases near the MPBL. This table provides, by column left to right, the following information: Date of cross spacecraft propagation detection and location; time of detection; two spacecraft on which the detection was made; lag time of detection of second spacecraft from the first as shown in previous column; pulse time duration of detected propagating ESWs; spacecraft separation parallel to the magnetic field; spacecraft separation perpendicular to the magnetic field; velocity of propagating ESWs; direction of propagation with respect to the earth; ESW size parallel to the magnetic field; and ESW size perpendicular to the magnetic field. Table 1 indicates that all of the ESWs except for the ones shown in Figure 1 are propagating toward the earth with velocities on the order of 1300-2400 km/s and sizes parallel and perpendicular to the magnetic field of 0.5-1.0 km and > than 40 km, respectively.

3. Modulation of ESWs

On March 3, 2002, around 22:00 UT the Cluster spacecraft were moving inbound toward Earth and located in the magnetosheath, crossing the magnetopause into the cusp around 22:03 UT and on into the magnetosphere/polar cap at about 22:57 UT based on the CIS ion and PEACE electron data. The crossing of these two boundaries took place during the long recovery phase of a Co-rotating Interaction Region/High Speed Stream (CIR/HSS) event. Figure 2 shows the total magnetic field magnitude, in nT, obtained from the FGM measurements (panel a) and the electron density obtained from Whisper measurements (panel b), both for Cluster spacecraft 3 (SC3) for the period 22:40 to 23:10 UT, thus encompassing the crossing into the polar cap from the magnetopause/cusp boundary at 22:57 UT. At the bottom of the figure is a listing of the spacecraft distance, R (in R_E), the magnetic local time, MLT (in hours), and the magnetic latitude, MLat (in degrees).

The focus of the current study is the time period 22:51 to 22:55 UT, during which time the modulated ESW bursts were detected almost continuously. In this period of time the electron density was ~10 cm^{-3} and the magnetic field strength was ~144 nT as seen in Figure 2. Based on these values we obtain an electron plasma frequency f_{pe} ~ 28.5 kHz, electron cyclotron frequency f_{ce} ~ 4 kHz, proton cyclotron frequency f_{cH+} ~ 2.2 Hz, He_+ cyclotron frequency, f_{cHe+} ~ 0.5 Hz, and O^+ cyclotron frequency f_{cO+} ~ 0.14 Hz. At this time SC3 was located in the magnetopause/cusp boundary layer just prior to crossing into the polar cap and magnetosphere proper at ~ 9 R_E, -74 degrees MLat and 14.7 hours MLT.

An example of the modulation of the ESWs observed during this period of time is shown in Figure 3. Figure 3b shows wavelet analysis of the WBD waveform data using a Morlet mother wavelet, which strongly resembles the ESWs pulses. The analyzed data cover an ~ 2.4 ms time interval (horizontal axis) vs. frequency as inverse wavelet time scale (vertical scale) in the range 62 Hz to 10 kHz with color indicating the power (intensity) of the waves in arbitrary units. We clearly see three bursts of electrostatic waves roughly in the band of ~ 0.2 to 4 kHz. Note that the broad frequency, intense signatures (red color) observed just before 0.4 and 2.0 s and centered at 1.4 s are artifacts of gain change ringing in the WBD receiver and should be ignored. Figure 3a shows a representative 20 ms waveform taken from one of the bursts observed in Figure 3b. One of the ESW pulses, of which there are four that are well defined, in this example, has a pulse duration on the order of 300 microseconds and an amplitude of ~ 0.64 mV/m peak-

to-peak as indicated in Figure 3a. Pulses such as this make up the electrostatic bursts observed in Figure 3b in the band of 0.2 to 4 kHz. These ESWs occur in bursts that are modulated at ~1.3 Hz (3 bursts in 2.4 seconds) as opposed to being continuously or randomly observed throughout the 2.4 ms time interval. Probably unrelated to the modulated ESWs is the presence of narrow-banded waves observed around 3.5 to 4.0 kHz (just below f_{ce}). Based on the sinusoidal nature of these waves observed in the WBD waveforms and on STAFF-SA data analysis showing these waves to be right-hand polarized, they are most likely whistler mode waves given their frequency.

Complementing these higher frequency wave observations are those of the STAFF-SC instrument onboard SC3 for the period from 22:45 to 23:00 UT in Figure 4. Panel a (top) shows the total power spectral density of the three components of the magnetic field. After filtering to retain the most energetic part of the spectrogram, we analyzed the wave properties with the singular value decomposition (SVD) method (Santolík et al., 2003) as follows. Theta (in degrees), the angle between the wave vector **k** and the magnetic field **B**, is shown in panel b with the blue color code meaning **k** and **B** are parallel. The sense of polarization is plotted in panel c with the blue and red colors meaning left- and right-hand polarization, respectively (see equation (4) of Santolík et al. (2001)). Ellipticity is shown in panel d with the blue and red colors meaning fully circular left- and right-handed waves, respectively. Panel e provides the coherency of the waves. A low coherency value (Santolík and Gurnett, 2002) indicates that there are random phase shifts between the two components in the polarization plane. For each panel, frequency is plotted on the vertical scale, ranging from 0.5 to 3.5 Hz, and the superimposed black line is the local proton cyclotron frequency.

The most striking feature observed in Figure 4, panel a, are the magnetic waves detected between 22:51 and 22:55 UT in the frequency range of about 1.2-1.7 Hz, which is greater than half of the local proton cyclotron frequency. Their intensity is larger than the background fluctuations by only about two orders of magnitude. Due to this relatively weak power and other electrostatic fluctuations, these waves are not well seen in the electric field data. Nevertheless, analysis of the Poynting flux using these data together with those shown in Figure 4 indicates that the energy of these waves is anti-parallel to the magnetic field (not shown). Thus, these waves are propagating along the magnetic field from lower latitudes. The low theta values of these waves (panel b) indicate that their transverse component is larger than that of the compressive one. The sense of polarization is mainly left hand but with some right-hand excursions (panel c). This observation when considered with the low absolute value of the ellipticity (panel d) suggests the simultaneous presence of both left- and right-handed waves. Since the coherency level is quite high (panel e), the polarization analysis can be trusted.

Given the properties of these waves and their frequency range, they are most likely EMIC waves of the unstructured Pc1 type (Jacobs et al., 1964; Hayashi et al., 1981; Fraser et al., 1984). The Pc1 waves observed in Figure 4 are relatively weak compared to those from a similar ESW modulation event observed on March 30, 2002 near the plasmapause boundary layer (see Pickett et al., 2010). Pc1 waves are expected to be present near the dayside magnetopause based on satellite and ground measurements (Anderson et al., 1992;1996; Neudegg et al., 2002). Although there is still some uncertainty as to why these Pc1 waves are found there, there is no question as to their presence just inside the magnetopause on this date. Furthermore, although we have presented a single event of ESW modulation near the magnetopause, several other events exist within the Cluster data set but no attempt has yet been made to correlate these with the presence of Pc1 waves.

4. Discussion

The ESW pulse durations, being on the order of 500 microseconds or less as shown in Table 1, are consistent with propagation speeds of electron holes measured on single spacecraft in this region (Cattell et al., 2002). Their pancake shape and characteristic size, which along the magnetic field is of the order

of 1 km or less and across the field of tens of km, are consistent with electron holes as well (Franz et al., 2000; Cattell et al., 2002). However, their characteristics are also consistent with electron acoustic solitons resulting from theoretical models for cusp and magnetosheath plasmas (Ghosh et al. 2008; Lakhina et al., 2009). Although we have been able to document propagation of ESWs across distances as great as tens of km near the magnetopause on the magnetosheath side by correlating a series of noncyclic ESW pulses across two different Cluster spacecraft, it was difficult and time-consuming to identify even the few cases shown in Table 1. Part of the difficulty is related to the fact that in most regions where ESWs are observed, i.e., boundary layers and turbulent regions, these regions are rich with other types of waves, some of which are of higher intensity, thus making it harder to isolate a series of ESWs for cross correlation analysis. Were we to cross correlate using only one isolated ESW pulse, we would have numerous correlations, almost all of which would be meaningless. This is because in any one region of space where ESW pulses are observed, they are usually numerous and of similar magnitudes and time duration as mentioned in Section 2. Obviously, the active physical processes which generate ESWs in any region of space at any given time will generate them with similar characteristics on an ongoing basis unless significant changes (currents, beams, density perturbations) in the plasma are introduced to either squelch those processes or change their characteristics due to those changes.

Our primary purpose in presenting results of propagation of ESWs was to demonstrate that nonlinear ESWs which are generated close to the magnetopause can in fact be stable for as long as 22 ms, as opposed to the relatively short time of ~ 0.1 ms observed on single spacecraft. This is a very long time considering the time scales of the ESWs themselves (few 100s of microseconds). Further, we have demonstrated that ESWs can propagate across great distances (tens of km), in relation to their sizes along the propagation direction (1 km or less), without being disturbed by other waves and particles. This is perhaps an unexpected result. However, when viewed in light of the analysis carried out by Chen et al. (2005) based on Polar data (Franz et al. 2005) , in which the widths and amplitudes of electron holes are found to be only loosely constrained, this implies the real possibility of spontaneous generation of phase-space holes in turbulent fluctuations and can play a role in transport and electrical conductivity in collisionless plasma processes such as magnetic reconnection and boundary formation. It remains an open problem to prove that ESWs are playing a role in these processes, but having information on the propagation and stability of ESWs in these boundary regions will help shed light on that problem.

With regard to the modulation of ESWs, we have seen in Section 3 that co-located Pc1 waves at this modulation frequency are certainly essential in explaining the modulation phenomenon. Since the electron plasma period (few tens of microseconds) is usually of a time scale that is less than but consistent with the ESWs observed in the region of space near the magnetopause (few 100s of microseconds), we now look to the electron data for help in determining the generation of the ESWs that would also be consistent with their modulation. Figure 5 shows a cross section of the energy distribution function from the PEACE instrument which was recorded during the time of the ESW modulation bursts shown in Figure 3. The color scale shows the number of counts accumulated over the time interval shown with energy plotted on the vertical and horizontal axes. The magnetic field direction is up (or vertical) in this figure. Here we clearly see that electron beams of a few tens of eV are observed at parallel and anti-parallel to the magnetic field and at ~ 45 degrees from the anti-parallel direction. These beams are persistent throughout the time of the observations of the modulated ESWs and Pc1 waves (~2251 to 2255 UT), while outside this interval the electrons are more isotropic and/or at higher energies.

The ion data obtained from the CIS instrument are also remarkable in that in the period when the modulated ESW bursts are observed the direction of the ion velocity shows a direction reversal without undergoing a significant change in magnitude. The direction of flow of the ~ 100 eV protons undergoes a change primarily in the Vx (GSE) direction from approximately -30 km/s to +20 km/s with the V_θ angle changing from -160 to -45 degrees and the V_φ from -55 to -85 degrees. It is possible that this change in direction is related to the presence of the Pc1 waves, just as the electron beams are present primarily

during this same interval of time. It is also possible that the ion flow direction has changed in response to the DC magnetic field pulse seen in Figure 2 during this 22:51-:22:55 UT time period or that it is expected as the spacecraft approaches the polar cap boundary layer from the magnetopause/cusp region.

We are left with the question of how the Pc1 waves might be affecting the plasma environment close to the magnetopause such that ESWs are generated in bursts at the Pc1 wave frequency and what role the electrons and ions play in the generation of these ESWs. In order to answer this question, we first point out one very important aspect of the Pc1 waves. These waves will have an electric field component which lies along the magnetic field direction. This was previously demonstrated, for example, by Tsurutani et al. (2003) using Polar data where an EMIC wave of similar frequency (~2.3 Hz, slightly below the local f_{cp} of 3.05 Hz) was found to be propagating obliquely to the magnetic field in a polar cap boundary layer. This region is very similar to the one discussed here for Cluster. The EMIC wave in the Polar study was found to have a measurable $E_{//}$ component. This $E_{//}$ component can give rise to strong electric currents (induced DC electric field). This electric field will then accelerate and beam thermal electrons along the magnetic field. Their drift velocity will exceed the thermal velocity of the ions, which allows the Buneman instability to take place (Omura et al., 2003). If Ti >> Te, this instability will lead to formation of ESWs through the coalescence of large electrostatic potentials, while if Ti << Te, ion acoustic waves will result. In the case under study, Ti and Te are approximately of the same order, but in any case, not significantly different. In this case, the ESWs are still formed but the amount of trapped electrons will be less (Omura et al. 2003) and thus the process less efficient at generating ESWs.

Lakhina et al. (2004) suggested that for the Polar observations presented by Tsurutani et al. (2003), the ESWs could have been generated through the bi-stream electron instability as discussed in Omura et al. (1996). The counter-streaming electron beams in this case arise through acceleration by the parallel electric field components of the obliquely-propagating ion cyclotron waves as suggested by Tsurutani et al. (2003). The analysis of Lakhina et al. (2004) showed that such beam modes would saturate by trapping electrons, thus producing bipolar pulses and electron holes. We also look back to the GEOS observations of Cornilleau-Wehrlin (1981) in which wide spectrum electrostatic waves which extended between the lower hybrid frequency and the ion plasma frequency were observed to be modulated at a ULF frequency around the helium gyrofrequency. The ULF-associated electrostatic waves were observed in the dayside region of the outer magnetosphere (L > 6) at all geomagnetic latitudes sampled by the GEOS satellites (< 30 degrees). Although the Cluster observations are at a much higher latitude, we believe that the phenomenon may be a similar one. The electrostatic waves observed by GEOS are clearly observed in a frequency range (hundreds of Hz) much lower than Cluster (several kHz). In addition, the waveforms were not available from which to determine whether ESW-type pulses were the primary constituent of those GEOS electrostatic waves. Nonetheless, Roux et al. (1984) postulated that electrons having parallel velocities that are close to the Alfven velocity at the equator can be trapped in the potential troughs of the ULF waves due to the small but finite parallel electric field developed by the ULF waves in a multi-component plasma,. The trapped electrons are accelerated along the magnetic field as the parallel phase velocity of the ULF waves increase as they leave the magnetic equator. They suggest that the freshly detrapped electrons, which were found by Mauk and McPherron (1980) to be modulated at the ULF frequency, are responsible for the ULF-modulated electrostatic waves. Thus, both the ULF waves and the ULF-modulated electrostatic waves can be observed simultaneously, through their connection with the accelerated electrons. It is beyond the scope of the present paper to carry out all of the necessary computations and models to determine the precise mechanism by which the Cluster ESWs are generated and modulated at the Pc1 wave frequency. However, as just discussed, the data support the suggestion that the $E_{//}$ component of the Pc1 waves initiates the process, setting up the conditions favorable for the Buneman instability to be initiated.

We would like to end our discussion of modulated ESWs by comparing our results to laboratory and space-based observations of whistler mode wave packets. We begin with the ISEE-1 and ISEE-2

observation that whistler mode chorus emissions in the earth's outer magnetosphere on the dayside are often accompanied by high-frequency bursts of electrostatic waves whose frequencies were slightly below the electron plasma frequency. High time resolution measurements of these bursts reveal that at certain times these bursts are modulated at the chorus frequency. Reinleitner et al. (1983) proposed a model in which the electrons are free to move along the ambient magnetic field line under the influence of the parallel electric field, $E_{//}$, of the chorus waves. This electric field permits electrons to be trapped in effective potential wells of the chorus wave and to be carried along with them at the chorus phase velocity, thus exciting electrostatic waves via a two steam instability. A similar example on Polar in the cusp turbulent boundary of electrostatic bursts modulated at a whistler mode frequency was consistent with the proposed mechanism as that for the ISEE observations (Pickett et al., 2001). Both of these cases are consistent with the initial instability being that of the Buneman instability as discussed by Omura et al. (2003) and with a high frequency instability discussed by Lakhina et al. (2003) with regard to the generation of ESWs in the polar cap boundary layer from Polar observations and which involved the $E_{//}$ component of EMIC or Alfven waves. Recent laboratory experiments in which a suprathermal electron beam injection into a laboratory plasma has led to the generation of ESWs and electrostatic whistler wave (EWW) packets (Lefebvre et al., 2010). The laboratory ESWs have time durations comparable to those derived from various observations of ESWs in the magnetosphere (e.g., Pickett et al., 2009). Further, these EWW packets have similar characteristics to those of the electrostatic bursts discussed by Reinleitner et al. (1983) and Pickett et al. (2001), both of which being associated with whistler mode waves. Although the Cluster-modulated ESW bursts discussed here do not appear to be associated with the whistler mode waves observed during the study event, but rather with a much lower frequency Pc1 wave similar to the Cornilleau-Wehrlin (1981) and Roux et al. (1983) events from GEOS, there is one common element tying all of these events together. All appear to depend on the $E_{//}$ component of an electromagnetic wave in the presence of the electrons, which allows the electrons to be accelerated through the Buneman instability.

5. Summary and Conclusions

We have shown that it is possible to detect ESW propagation across distances of a few tens of km using multi-spacecraft Cluster observations near the dayside magnetopause on the magnetosheath side. However, very few cases were found by using cross spacecraft waveform correlation techniques carried out on a computer with follow-up visual confirmation. The cases of high correlation were listed in Table 1 with their characteristic propagation speeds and sizes. These characteristics are similar to many electron holes and electron acoustic solitons previously reported in the literature, and help to confirm that our method for cross correlation is reliable. The primary conclusion we draw from this analysis is that ESWs can be stable over distances as great as tens of km and for time periods on the order of 22 ms and greater near the magnetopause. This is a very significant aspect of ESWs that needs to be considered when developing theories for how ESWs interact with particles and waves and contribute to the bulk properties of the plasmas in which they are found.

Our study of the modulation of the ESW bursts near the dayside magnetopause on the Earth side has found that these bursts occur at the same frequency as a concurrently observed Pc1 wave at 1.2 – 1.7 Hz. This Pc1 wave will have a measurable electric field component parallel to the magnetic field which acts as an induced electric field. This induced electric field allows for the acceleration of electrons and ions along the local magnetic field as the PC1 wave propagates, setting up the necessary conditions for the initiation of a Buneman type instability. This instability has been shown in previous theoretical and observational work to lead to the generation of ESWs, which would be modulated at the frequency of the wave that led to the initiation of the Buneman instability, i.e., the Pc1 waves for our event. Although we have presented data showing all of the necessary conditions are present to lead to these conclusions, it is an empirical result which needs to be investigated in more detail through theory and modeling. Furthermore, the possibility that most of the modulated ESW events reported in the literature in

association with Pc1 waves observed in space are related to the modulated electrostatic wave bursts reported in the literature in association with whistler mode waves needs to be studied further since all cases seem to suggest that the $E_{//}$ component for accelerating particles is common across all these cases. Finally, studying all of these events with those from the laboratory in which ESWs and EWWs are produced will help us in understanding the various generation mechanisms of ESWs and where these mechanisms are likely to be active in space.

Acknowledgments

This work was supported at The University of Iowa by NASA GSFC under Grant NNX07AI24G, and at Augsburg College under NSF grant ATM-0827903. The Cluster Active Archive (CAA) is acknowledged for supplying the EFW low frequency electric field data referred to in this article. JSP thanks the organizing committee for inviting her to give a presentation of this work honoring the career of Dennis Papadopoulos at the conference "Modern Challenges in Nonlinear Plasma Physics".

References

Anderson, B. J., R. E. Erlandson, and L. J. Zanetti (1992), A statistical study of Pc 1-2 magnetic pulsations in the equatorial magnetosphere 1. Equatorial occurrence distributions, *J. Geophys. Res.*, *97*, 3075-3088.

Anderson, B. J., E. R. Erlandson, M. J. Engebretson, J. Alford, and R. L. Arnoldy (1996), Source region of 0.2 to 1.0 Hz geomagnetic pulsation bursts, *Geophys. Res. Lett.*, *23*, 769-772.

Balogh, A., M. W. Dunlop, S. W. Cowley, D. J. Southwood, J. Thomlinson, J., et al.: The Cluster Magnetic Field Experiment, Space Sci. Rev., 79, 65-91, 1997.

Chen, Li-Jen, Jolene Pickett, Paul Kintner, Jason Franz, and Donald Gurnett (2005), On the width-amplitude inequality of electron phase space holes, *J. Geophys. Res.*, *110*, A09211, doi:10.1029/2005JA011087.

Cattell, C., J. Crumley, J. Dombeck, J. Wygant, and F. S. Mozer (2002), Polar observations of solitary waves at the Earth's magnetopause, *Geophys. Res. Lett.*, *29*, 1065, 10.1029/2001GL014046.

Cornilleau-Wehrlin, N. (1981), A new ULF-modulated electrostatic wave detected in the extremely low frequency range onboard Geos, *J. Geophys. Res.*, *86*, 1365-1373.

Cornilleau-Wehrlin, N., G. Chanteur, S. Perraut, L. Rezeau, P. Robert, et al. (2003), First results obtained by the Cluster STAFF experiment, *Ann. Geophys.*, *21*, 437-456.

Décréau, P. M. E., P. Fergeau, V. Krannosels'kikh, M. Lévêque, Ph. Martin, et al. (1997), Whisper, A resonance sounder and wave analyzer: performances and perspectives for the Cluster mission, *Space Sci. Rev.*, *79*, 157-193.

Franz, J. R., P. M. Kintner, and J. S. Pickett (1998), POLAR observations of coherent electric field structures, *Geophys. Res. Lett.*, *25*, 1277-1280.

Franz, J. R., P. M. Kintner, C. E. Seyler, J. S. Pickett, and J. D. Scudder (2000), On the perpendicular scale of electron phase-space holes, Geophys. Res. Lett., 27, 169-172.

Franz, J. R., P. M. Kintner, J. S. Pickett, L.-J. Chen (2005), Properties of small amplitude electron phase-space holes observed by Polar, *J. Geophys. Res.*, *110*, A09212, doi:10.1029/2005JA011095.

Fraser, B. J., W. J. Kemp, and D. J. Webster (1984), Pc1 pulsation source regions and their relationship to the plasmapause, *Eur. Space Agency Spec. Publ., ESA SP-217*, 609-613.

Ghosh, S. S., J. S. Pickett, G. S. Lakhina, J. D. Winningham, B. Lavraud, B. and P. M. E. Décréau (2008), Parametric analysis of positive amplitude electron acoustic solitary waves in a magnetized plasma and its application to boundary layers, *J. Geophys. Res.*, *113*, A06218, doi:10.1029/2007JA012768.

Gurnett, D. A., R. L. Huff, and D. L. Kirchner (1997), The Wide-Band Plasma Wave Investigation, *Space Sci. Rev.*, *79*, 195-208.

406 Hayashi, K., T. Kokubun, T. Oguti, K. Tsuruda, S. Machida, T. Kitamura, O. Saka, and T. Watanabe
407 (1981), The extent of Pc1 source region in high latitudes, *Can. J. of Phys., 69*, 1097-1105.
408 Jacobs, J. A., Y. Kato, S. Matsushita, and V. A. Troitskaya (1964), Classification of geomagnetic
409 micropulsations, *J. Geophys. Res., 69*, 180.
410 Johnstone, A. D., C. Alsop, P. J. Carter, A. J. Coates, A. J. Coker, et al. (1997), PEACE: A plasma
411 electron and current experiment, *Space Sci. Rev.*, *79*, 351-398.
412 Lakhina, G. S., B. T. Tsurutani, and J. S. Pickett (2004), Association of Alfvén waves and proton
413 cyclotron waves with electrostatic bipolar pulses: magnetic hole events observed by Polar, *Nonlin.*
414 *Proesses. Geophys*., *11*, 205-213.
415 Lakhina, G. S., S. V. Singh, A. P. Kakad, M. L. Goldstein, A. F. Viñas, and J. S. Pickett (2009), A
416 mechanism for electrostatic solitary structures in the Earth's magnetosheath, *J. Geophys. Res.*, *114*,
417 A09212, doi:10.1029/2009JA014306.
418 Lefebvre, Bertrand, Li-Jen Chen, Walter Gekelman, Paul Kintner, Jolene Pickett, Patrick Pribyl, Stephen
419 Vincena, Franklin Chiang, and Jack Judy (2010), Laboratory measurements of electrostatic solitary
420 structures generated by beam injection, *Phys. Rev. Lett.*, *submitted*.
421 Matsumoto, H., H. Kojima, T. Miyatake, Y. Omura, M. Okada, et al. (1994), Electrostatic solitary waves
422 (ESW) in the magnetotail: BEN wave forms observed by GEOTAIL, *Geophys. Res. Lett.*, *21*, 2915–
423 1918.
424 Matsumoto, H., X. H. Deng, H. Kojima, and R. R. Anderson (2003), Observation of electrostatic solitary
425 waves associated with reconnection on the dayside magnetopause boundary, *Geophys. Res. Lett.*, *30*,
426 1326, doi:10.1029/2002GL016319.
427 Mauk, B. H., and R. L. McPherron (1980), An experimental test of the electromagnetic ion cyclotron
428 instability with the earth's magnetosphere, *Phys. Fluids*, *23*, 2111-2127.
429 Neudegg, D. A., B. J. Fraser, F. W. Menk, G. B. Burns, R. J. Morris, and M. J. Underwood (2002),
430 Magnetospheric sources of Pc1-2 ULF waves observed in the polar ionospheric waveguide (2002),
431 *Antarctic Science*, *14(1)*, 93-103.
432 Omura, Y., H. Matsumoto, T. Miyake, and H. Kojima (1996), Electron beam instabilities as generation
433 mechanisms of electrostatic solitary waves in the magnetotail, *J. Geophys. Res.*, *101*, 2685-2697.
434 Omura, Y., W. J. Heikkila, T. Umeda, K. Ninomiya, and H. Matsumoto (2003), Particle simulation of
435 plasma response to an applied electric field parallel to magnetic field lines, J. Geophys. Res., 108,
436 1197, doi:10.1029/2002JA009573.
437 Pickett, J. S., J. R. Franz, J. D. Scudder, J. D. Menietti, D. A. Gurnett, G. B. Hospodarsky, R. M.
438 Braunger, P. M. Kintner, and W. S. Kurth (2001), Plasma waves observed in the cusp turbulent
439 boundary layer: An analysis of high time resolution wave and particle measurements from the Polar
440 spacecraft, *J. Geophys. Res.*, *106*, 19,081-19,099.
441 Pickett, J. S., L.-J. Chen, S. W. Kahler, O. Santolík, D. A. Gurnett, D. A., et al. (2004a), Isolated
442 electrostatic structures observed throughout the Cluster orbit: Relationship to magnetic field strength,
443 *Annales Geophys., 22*, 2515-2523.
444 Pickett, J. S., S. W. Kahler, L.-J. Chen, R. L. Huff, O. Santolík, et al. (2004b), Solitary waves observed in
445 the auroral zone: the Cluster multi-spacecraft perspective, *Nonlin. Processes Geophys.*, *11*, 183-196.
446 Pickett, J. S., L.-J. Chen, R. L. Mutel, I. W. Christopher, O. Santolík, O., et al. (2008), Furthering our
447 understanding of electrostatic solitary waves through Cluster multispacecraft observations and theory,
448 *Adv. Space Res.*, *41*, 1666-1676.
449 Pickett, J. S., L.-J. Chen, O. Santolík, S. Grimald, B. Lavraud, et al. (2009), Electrostatic solitary waves in
450 current layers: from Cluster observations during a super-substorm to beam experiments at the LAPD,
451 *Nonlin. Processes Geophys.*, *16*, 431-442.
452 Pickett, J. S., B. Grison, Y. Omura, M. J. Engebretson, I. Dandouras, A. Masson, M. L. Adrian, O.
453 Santolik, P. M. E. Decreau, N. Cornilleau-Wehrlin, and D. Constantinescu (2010), Cluster
454 observations of EMIC chorus emissions in association with Pc1 waves near Earth's plasmapause,
455 *Geophys. Res. Lett.*, *submitted*.

Reinleitner, Lee, Donald A. Gurnett, and Timothy E. Eastman (1983), Electrostatic bursts generated by electrons in Laundau resonance with whistler mode chorus, *J. Geophys. Res.*, *88*, 3079-3093.

Rème, H., C. Aoustin, J. M. Bosqued, I. Dandouras, B. Lavraud, et al. (2001), First multispacecraft ion measurements in and near the Earth's magnetosphere with the identical Cluster ion spectrometry (CIS) experiment, *Ann. Geophys.*, *19*, 1303-1354.

Roux, A., N. Cornilleau-Wehrlin, and J. L. Rauch (1984), Acceleration of thermal electrons by ICW's propagating in a multicomponent magnetospheric plasma, *J. Geophys. Res.*, *89*, 2267-2273.

Santolik, O., F. Lefeuvre, M. Parrot, and J. L. Rauch (2001), Complete wave-vector directions of electromagnetic emissions : Application to INTERBALL-2 measurements in the nightside auroral zone, *J. Geophys. Res.*, *106*, 13,191-13,201.

Santolik, O., and D. A. Gurnett (2002), Propagation of auroral hiss at high altitudes, *Geophys. Res. Lett.*, *29(10)*, 1481, doi:10.1029/2001GL013666.

Santolik, O., M. Parrot, and F. Lefeuvre (2003), Singular value decomposition methods for wave propagation analysis, Radio Sci., 38(1), 1010, doi:10.1029/2000RS002523.

Temerin, M., K. Cerny, W. Lotko, and F. S. Mozer (1982), Observations of double layers and solitary waves in the auroral plasma, *Phys. Rev. Lett.*, *48*, 1175–1179, 1982.

Tsurutani, B. T., B. Dasgupta, J. K. Arballo, G. S. Lakhina, and J. S. Pickett (2003), magnetic field turbulence, electron heating, magnetic holes, proton cyclotron waves, and the onsets of bipolar pulse (electron hole) events: a possible unifying scenario, *Nonlin. Processes Geophys.*, *21*, 27-35.

Figure Captions

Figure 1: Example of ESW propagation from Cluster SC4 to SC3 where the SC3 waveforms have been brought forward in time by the detected lag to SC4 (22.49 ms) and overlaid on the SC4 waveforms. (Extracted from Figure 5 of Pickett et al., 2008).

Figure 2: Magnetic field strength and density measurements on Cluster 3 while the spacecraft is in the magnetopause boundary layer on the earthward side.

Figure 3: (a) Example of ESWs detected on Cluster 3. (b) Wavelet spectrogram showing bursts of electrostatic waves in the frequency range 0.2 -4 kHz and narrow-banded waves (probably whistler mode) around 3.5 – 4.0 kHz. The electrostatic bursts are comprised of ESWs as shown by the location of the waveform sample in Figure 3(a).

Figure 4: (a) Magnetic field spectral measurements in the frequency range 0.5 to 3.5 Hz showing the presence of Pc1 waves around 1.2 – 1.7 Hz from 22:51 to 22:55 UT. (b) Theta angle of the k vector; (c) Polarization of the waves; (d) Ellipticity of the waves; and (e) coherency of the waves, using the SVD method as applied to the data plotted in panel (a).

Figure 5: Cross section of the electron energy distribution function during the ESW measurements shown in Figure 3(a). Electron beams of a few tens of eV are present at parallel and antiparallel to the local magnetic field, as well as at 45 degrees to magnetic field direction.

Table 1: Characteristics of ESWs obtained through cross spacecraft waveform correlations

Date (Year/Month/ Day)	Time (UT)	Cluster space-craft	Lag (ms)	Pulse Duration (ms)	$D_{B//}$ (km)	$D_{B\perp}$ (km)	Velocity (km/s)	Direction (referenced to Earth)	$L_{B//}$ (km)	$L_{B\perp}$ (km)
2002/02/19 11.84 R_E 13.53 MLT -53.9 MLat	22:20:27.90	4,3	22.5	0.60	30	40	1,334	Away	0.8	≥40
2002/04/03 11.79 R_E 10.85 MLT -52.5 MLat	18:00:54.54	2,1	19.5	0.30	38	95	1,947	Toward	0.6	≥95
2002/05/04 13.32 R_E 08.25 MLT -42.4 MLat	14:02:57.11	4,1	37.8	0.25	71	79	1,870	Toward	0.5	≥79
2002/05/04 13.26 R_E 08.27 MLT -42.6 MLat	14:08:06.19	3,1	15.6	0.30	37	97	2,365	Toward	0.7	≥97
2002/05/04 13.26 R_E 08.27 MLT -42.6 MLat	14:08:06.20	3,1	17.0	0.45	37	97	2,167	Toward	1.0	≥97
2002/05/04 13.26 R_E 08.27 MLT -42.6 MLat	14:08:06.23	3,1	21.4	0.37	37	97	1,724	Toward	0.6	≥97

2002/02/19

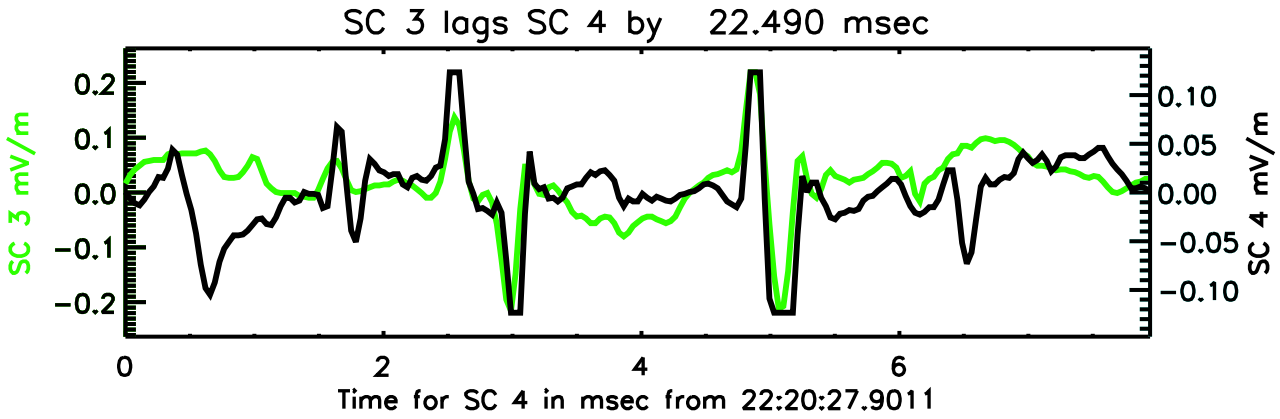

Figure 1

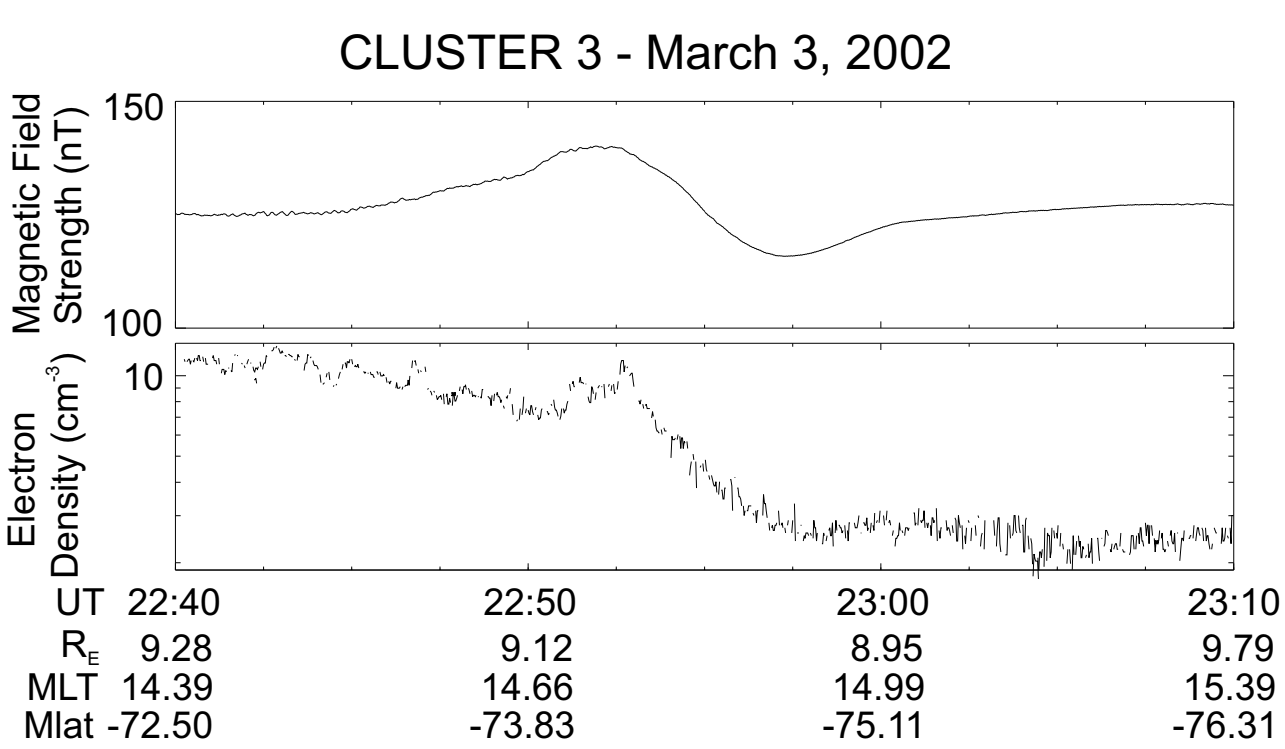
CLUSTER 3 - March 3, 2002
Magnetic Field Strength (nT)
150
100
Electron Density (cm-3)
10
UT 22:40 22:50 23:00 23:10
RE 9.28 9.12 8.95 9.79
MLT 14.39 14.66 14.99 15.39
Mlat -72.50 -73.83 -75.11 -76.31

Figure 2

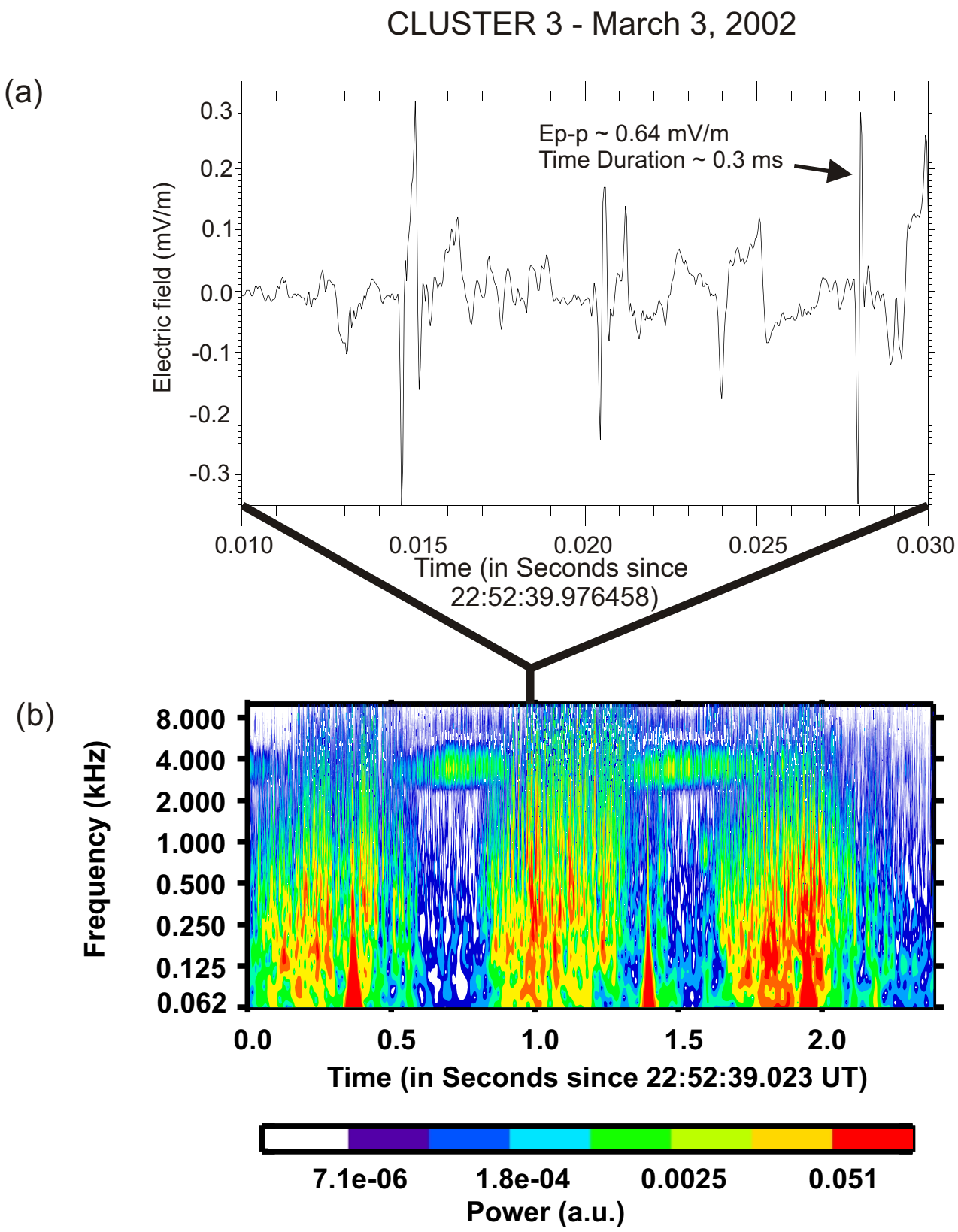
CLUSTER 3 - March 3, 2002
(a)
Ep-p ~ 0.64 mV/m
Time Duration ~ 0.3 ms
Electric field (mV/m)
0.3
0.2
0.1
0.0
-0.1
-0.2
-0.3
0.010
0.015
0.020
0.025
0.030
Time (in Seconds since 22:52:39.976458)
(b)
Frequency (kHz)
8.000
4.000
2.000
1.000
0.500
0.250
0.125
0.062
0.0
0.5
1.0
1.5
2.0
Time (in Seconds since 22:52:39.023 UT)
7.1e-06
1.8e-04
0.0025
0.051
Power (a.u.)

Figure 3

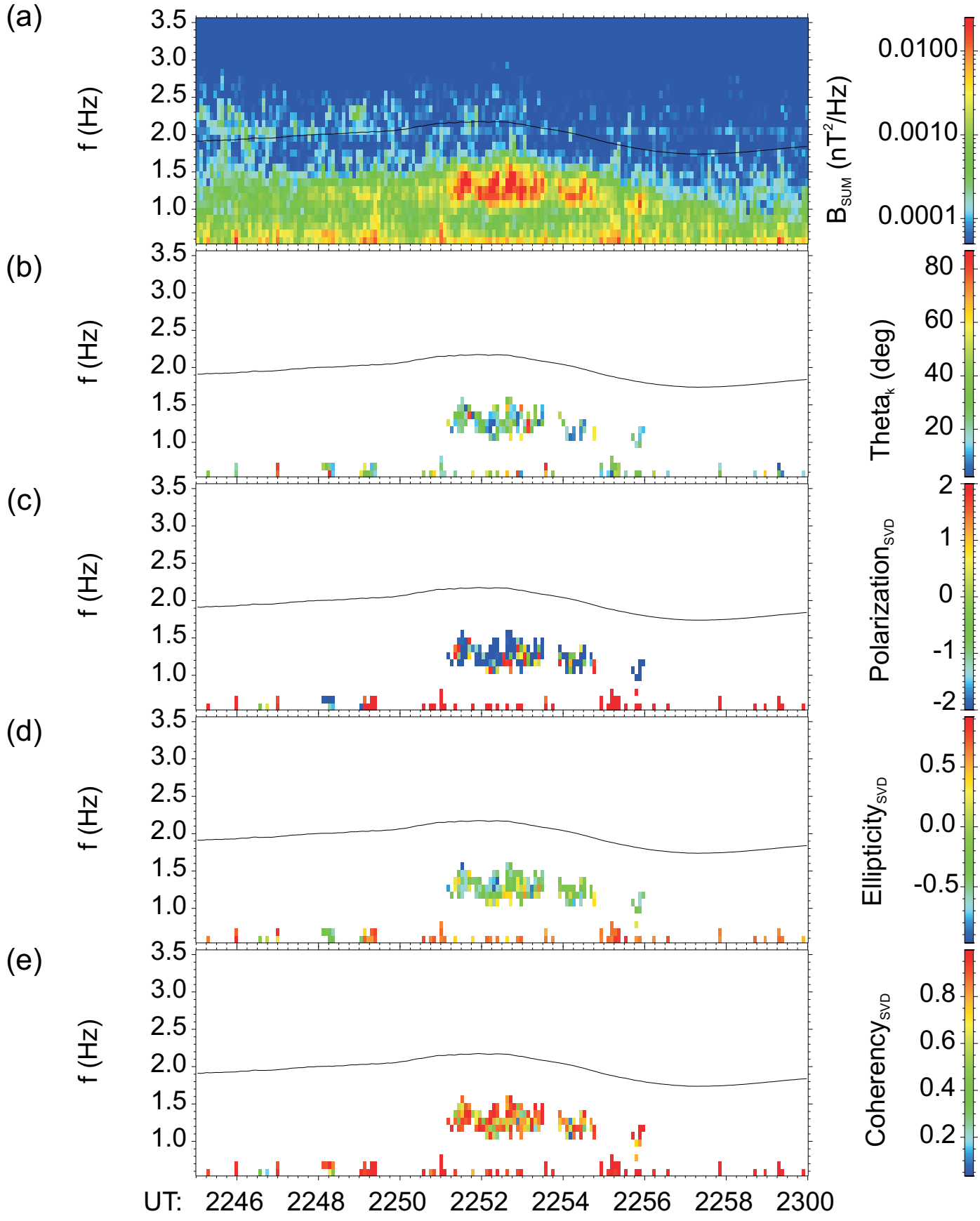
CLUSTER 3 - March 3, 2002
(a)
(b)
(c)
(d)
(e)
f (Hz)
3.5
3.0
2.5
2.0
1.5
1.0
UT:
2246
2248
2250
2252
2254
2256
2258
2300
B_SUM (nT²/Hz)
0.0100
0.0010
0.0001
Theta_k (deg)
80
60
40
20
Polarization_SVD
2
1
0
-1
-2
Ellipticity_SVD
0.5
0.0
-0.5
Coherency_SVD
0.8
0.6
0.4
0.2

Figure 4

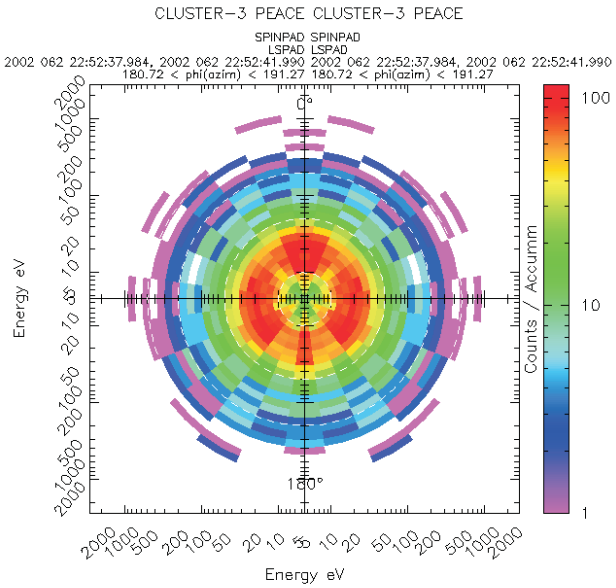
CLUSTER-3 PEACE CLUSTER-3 PEACE
SPINPAD SPINPAD
LSPAD LSPAD
2002 062 22:52:37.984, 2002 062 22:52:41.990 2002 062 22:52:37.984, 2002 062 22:52:41.990
180.72 < phi(azim) < 191.27 180.72 < phi(azim) < 191.27
0°
180°
Energy eV
Energy eV
Counts / Accumm
100
10
1

Figure 5